Published in final edited form as:
Aquat Toxicol. 2010 July 1; 98(3): 245–255. doi:10.1016/j.aquatox.2010.02.020.

Two farnesoid X receptor alpha isoforms in Japanese medaka (*Oryzias latipes*) are differentially activated *in vitro*

Deanna L. Howarth[1,§], **Lee R. Hagey**[2], **Sheran H.W. Law**[3], **Ni Ai**[4], **Matthew D. Krasowski**[5], **Sean Ekins**[4,6,7], **John T. Moore**[8], **Erin M. Kollitz**[3], **David E. Hinton**[1], and **Seth W. Kullman**[3,*]

[1]Integrated Toxicology and Environmental Health Program and Nicholas School of the Environment and Earth Sciences, Duke University, Durham, NC 27708, USA

[2]Department of Medicine, University of California at San Diego, La Jolla, CA 92093, USA

[3]Department of Environmental and Molecular Toxicology, North Carolina State University, Raleigh, NC 27695, USA

[4]Department of Pharmacology, Robert Wood Johnson Medical School, University of Medicine and Dentistry of New Jersey, Piscataway, NJ 08854, USA

[5]Department of Pathology, University of Iowa Hospitals and Clinics, Iowa City, IA, USA

[6]Collaboration in Chemistry, Jenkintown, PA 19046, USA

[7]Department of Pharmaceutical Sciences, University of Maryland, Baltimore, MD 21201, USA

[8]GlaxoSmithKline Discovery Research, Research Triangle Park, NC 27709, USA

Abstract

The nuclear receptor farnesoid X receptor alpha (FXRα, NR1H4) is activated by bile acids in multiple species including mouse, rat, and human and in this study we have identified two isoforms of Fxrα in Japanese medaka (*Oryzias latipes*), a small freshwater teleost. Both isoforms share a high amino acid sequence identity to mammalian FXRα (~70% in the ligand-binding domain). Fxrα1 and Fxrα2 differ within the AF1 domain due to alternative splicing at the fourth intron-exon boundary. This process results in Fxrα1 having an extended N-terminus compared to Fxrα2. A Gal4DBD-FxrαLBD fusion construct was activated by chenodeoxycholic, cholic, deoxycholic and lithocholic acids, and the synthetic agonist GW4064 in transient transactivation assays. Activation of the Gal4DBD-FxrαLBD fusion construct was enhanced by addition of PGC-1α, as demonstrated through titration assays. Surprisingly, when the full-length versions of the two Fxrα isoforms were compared in transient transfection assays, Fxrα2 was activated by C_{24} bile acids and GW4064, while Fxrα1 was not significantly activated by any of the compounds tested. Since the only significant difference between the full-length constructs was sequence in the AF1 domain, these experiments highlight a

*To whom correspondence should be addressed, at the Department of Environmental and Molecular Toxicology, North Carolina State University, PO Box 7633, Raleigh, NC 27695, USA. swkullma@ncsu.edu; Phone: 919-515-4378; Fax: 919-515-7169.
§Present address: Department of Medicine, Division of Liver Diseases and Department of Developmental and Regenerative Biology, Mount Sinai School of Medicine, 1 Gustave L. Levy Place, New York, NY 10029

DISCLAIMER The research described in this paper has been funded wholly or in part by the United States Environmental Protection Agency (EPA) under the Science to Achieve Results (STAR) Graduate Fellowship Program. EPA has not officially endorsed this publication and the views expressed herein may not reflect the views of the EPA.

key functional region in the Fxrα AF1 domain. Furthermore, mammalian two-hybrid studies demonstrated the ability of Fxrα2, but not Fxrα1, to interact with PGC-1α and SRC-1, and supported our results from the transient transfection reporter gene activation assays. These data demonstrate that both mammalian and teleost FXR (Fxrα2 isoform) are activated by primary and secondary bile acids.

INTRODUCTION

The nuclear receptor (NR) superfamily consists of a variety of ligand-activated transcription factors that modulate gene expression in conjunction with numerous coactivators and corepressors. The importance of NRs in cellular signaling is evident by their involvement in gene expression pathways spanning a wide variety of physiological processes (Germain et al. 2006). The NR family has been defined in multiple completed genomes: 48 in humans, 49 in mice, 68 and 72 in the pufferfishes (*Takifugu rubripes* and *Tetraodon nigroviridis*, respectively), 70 in zebrafish (Danio rerio), 71 in medaka (*Oryzias latipes*) (Kullman, personal communication) and over 270 in the nematode, *Caenorhabditis elegans* (Maglich et al. 2003; Bertrand et al. 2007; Metpally et al. 2007). Hormones such as retinoids, thyroid hormone, and steroids activate many of these proteins, while others are considered “orphan receptors” as their natural ligands have yet to be discovered. In some instances, however, ligands for some of these NRs such as fatty acids, oxysterols, and bile acids have been identified, resulting in their “adoption” (Makishima et al. 1999; Parks et al. 1999; Edwards et al. 2002).

One “adopted” NR is the farnesoid X receptor (FXRα), which is essential to bile acid (BA) homeostasis. Once considered an orphan receptor with no known endogenous ligand (Forman et al. 1995), it was later found to bind BAs such as chenodeoxycholic acid (CDCA), lithocholic acid (LCA), and cholic acid (CA) with high affinity, thus establishing its role as a bile acid receptor (BAR) (Makishima et al. 1999; Parks et al. 1999; Wang et al. 1999). Binding of a BA to FXRα activates the NR, which interacts with IR-1 response elements in target genes as a heterodimer with RXR. FXRα can regulate BA homeostasis through modulation in expression of small heterodimer partner (SHP) and it, in turn, represses the transcription of genes involved in both BA synthesis, such as CYP7A1 and CYP8B1 (Goodwin et al. 2000; Lu et al. 2000), and in BA transport, such as sodium taurocholate cotransporting polypeptide (NTCP), which moves recirculating BAs from portal blood into hepatocytes (Denson et al. 2001). Furthermore, FXRα directly enhances expression of bile salt export pump (BSEP), a transport protein that moves bile acids from the hepatocyte into canaliculi for transport out of the liver (Plass et al. 2002; Zollner et al. 2003). This function can potentially be exploited for alleviation of cholestatic liver disease through synthetic agonists such as GW4064 (Maloney et al. 2000; Liu et al. 2003). In mammals, four isoforms of FXRα exist, differing in both the sequence of the hinge region, and in the length of the AF1 region (Huber et al. 2002). A second FXR, FXRß (NR1H5), has been identified in mice and is activated by the cholesterol precursor lanosterol. This gene is separate from FXRα with its own gene locus, and should not be confused with the multiple splice variants of FXRα found in mammals. FXRß is also functional in dogs, but encodes a pseudogene in humans and primates (Otte et al. 2003). Recently a beta form of FXR was discovered in the little skate (*Leucoraja erinacea*) that is partially activated by BAs and scymnol sulfate, a major component of skate bile (Karlaganis et al. 1989; Cai et al. 2007). Interestingly, no ortholog to FXRα was identified in this species. The identification of an FXRß ortholog in the little skate suggests that this nuclear receptor arose early in evolution. It is possible that FXRα arose in response to the development of BA metabolism, generating ligand specificity based upon organismal necessities (Cai et al. 2007). This is evident throughout metazoans, as illustrated by the identification of DAF-12, a nuclear receptor that binds BA-like steroids and retains a high degree of sequence homology to the NR1I subfamily in *C. elegans* (Gerisch et al. 2007). This idea is also supported by recent findings with zebrafish

FXRα, which demonstrated its activation not by BAs but by C_{27} bile alcohols such as cyprinol sulfate, its major bile constituent (Goto et al. 2003; Reschly et al. 2008). Despite these findings, little is known regarding the evolution and function of FXRα in non-mammalian vertebrates.

Research from our laboratory has focused on the structural and functional characterization of a teleost biliary system, demonstrating the presence of a hexagonal network of canaliculi and bile preductules through *in vivo*, three-dimensional reconstructions (Hardman et al. 2007). However, information regarding the molecular mechanisms underlying proper hepatobiliary function in these species is sparse. Additional information of this nature is critical to form the basis for application of teleost liver studies to the analysis of toxicants and their metabolites which are removed from the organism via the biliary system. Herein we describe the isolation and functional characterization of two FXRα isoforms from a model teleost, the Japanese medaka (*Oryzias latipes*). Medaka have a rich history as a research model in chronic liver toxicity studies wherein the major focus was structural alteration (Braunbeck et al. 1992; Okihiro and Hinton 1999; Liu et al. 2003). The focus of this study was to establish the function of FXRα as a BA sensor in this model organism, and to create the initial molecular underpinnings necessary for the understanding of overall medaka hepatobiliary function.

MATERIALS and METHODS

Chemicals

Commercially available bile acids, TTNPB, 9-*cis* retinoic acid (RA), all-*trans* RA, and 17ß-estradiol were obtained from Sigma (St. Louis, MO). Dihydrotestosterone (DHT) and dehydroepiandrosterone (DHEA) were obtained from Steraloids (Newport, RI). GW4064 was graciously provided by Dr. Steven Kliewer (University of Texas Southwestern Medical Center). Stock solutions of these compounds were made in HPLC-grade DMSO (Mallinckrodt Chemicals, Hazelwood, MO).

Test animals

Treatment and handling of the test animals were in accordance with regulations mandated by the Duke University and North Carolina State University Institutional Animal Care and Use Committees (IACUC). Colonies of STII (see-through) and OR (orange-red) medaka were housed under recirculating freshwater aquaculture conditions. STII medaka from our colony were originally obtained from Y. Wakamatsu, Nagoya University, Japan (Wakamatsu et al. 2001). Water temperature and pH were monitored daily and maintained at ~22–25°C and ~7.4, respectively, and the fish were kept under a defined light-dark cycle (16 hours light, 8 hours dark). Dry food (Otohime B1, Reed Mariculture, Campbell, CA) was fed several times per day through automated feeders, and newly-hatched *Artemia* was fed once per day.

Total RNA isolation

Livers (3–4) were dissected from anesthetized adult male STII medaka and snap frozen in liquid nitrogen. The pooled livers were homogenized in 1 mL RNA-Bee (TelTest, Friendswood, TX) using a Polytron homogenizer (Kinematica, Lucerne, Switzerland) cleaned with RNase ZAP (Sigma), diethylpyrocarbonate (DEPC, Sigma)-treated sterile water, and sterile deionized water. Total RNA from the homogenized livers was isolated as described previously (Volz et al. 2005). DNA contamination was removed via on-column digestion using Qiagen RNase Free DNase as directed by the manufacturer (Qiagen, Valencia, CA). RNA was eluted with 30 μL RNase free water at 52°C and quantity and purity (260/280 ratio) measured using a NanoDrop® ND-1000 (NanoDrop, Wilmington, DE) spectrophotometer.

cDNA synthesis

First-strand cDNA was produced using 2 μg total liver RNA (isolated as previously described) diluted in RNase-free water to a total volume of 10 μL, 1 μL oligo(dT)$_{15}$ (Promega, Madison, WI) and 1 μL 10 mM dNTPs (Invitrogen, Carlsbad, CA) to a final volume of 12 μL. This mixture was heated to 65°C for 5 min and chilled for 2 min on ice. After centrifugation, 4 μL 5× first-strand buffer (Invitrogen), 2 μL 0.1 M dithiothreitol (DTT, Invitrogen) and 1 μL RNase OUT Inhibitor (40 U/μL, Invitrogen) were added to the reaction which was heated to 37°C. After a two min incubation, 1 μL Superscript Reverse Transcriptase (SS RT, 200 U/μL, Invitrogen) was added and incubated at 37°C for 1 hr, to allow for complete mRNA reverse-transcription. SS RT was heat-inactivated by incubation at 70°C for 15 min. All cDNA was stored at −20°C until use.

Fxrα1 isolation

Medaka *fxrα1* was identified through a BLAST search of the published medaka genome (URL: http://dolphin.lab.nig.ac.jp/medaka/index.php), using the associated gene prediction tool, with mouse FXRα as the reference sequence (GI: 6677831). The predicted sequence was amplified by PCR using the primers shown in Table 1 and Advantage 2 Taq from Clontech (Mountain View, CA) per the manufacturer's instructions.

Following PCR amplification, the resulting product (~1500 bp in length, determined via 1% agarose gel electrophoresis and visualization with ethidium bromide, not shown) was inserted into the pCR 2.1 vector through the TOPO TA Cloning system (Invitrogen) and transformed into chemically competent TOP10 *E. coli* (Invitrogen), following manufacturer's protocols. Positive colonies (medFXRα1/pCR 2.1) were selected via blue/white screening and cultured in LB-amp broth (Luria-Burtani, 150 μg/mL ampicillin) overnight at 37°C/200 rpm. Plasmid DNA was isolated from the cultures via the Qiagen Spin Miniprep Kit as per the manufacturer's instructions and sequenced in both directions.

5' RACE and medFXRα2 isolation

To obtain the 5' UTR of medFXRα1 cDNA, 5' RACE PCR was performed using the Marathon cDNA Amplification Kit (Clontech). Total RNA was extracted from brain, testis, gut and liver of medaka and used for poly (A)$^+$ mRNA purification in a ratio amount of 1:2:2:5, respectively. One microgram of poly (A)$^+$ mRNA was used as the source of RNA template. Nested primers for Fxrα1 were used in PCR (5' RACE 1 and 5' RACE 2) in accordance with the manufacturer's protocols. PCR products were visualized via 1% agarose gel electrophoresis with ethidium bromide. The two bands present in the gel were individually purified using the Promega Wizard SV Gel and PCR Cleanup Kit, inserted into the pCR 2.1 vector, transformed, cultured, isolated and bi-directionally sequenced. In this manner the 5' end of *fxrα2* was located. A primer for the 5' end (also containing an *Eco*RI restriction site, EcoRI-Fxrα2 Fwd) was created and used with a primer for the 3' end of Fxrα1 containing a restriction site for *Bam*HI to isolate the entire sequence of Fxrα2 (BamHI-Fxrα2 Rev). PCR was employed to isolate Fxrα2 in liver cDNA using Advantage 2 Taq (Clontech) as described for Fxrα1. Following PCR amplification, the resulting product (~1400 bp in length, determined via 1% agarose gel electrophoresis and visualization with ethidium bromide, not shown) was inserted into the pCR 2.1 vector through the TOPO TA Cloning system (Invitrogen) and transformed into chemically competent TOP10 *E. coli* (Invitrogen) following the manufacturer's protocols. Positive colonies (Fxrα2/pCR 2.1) were selected via blue/white screening and cultured in LB-amp broth (Luria-Burtani, 150 μg/mL ampicillin) overnight at 37°C/200 rpm. Plasmid DNA was isolated from the cultures via the Qiagen Spin Miniprep Kit as per the manufacturer's instructions and sequenced in both directions.

FXRα isoform expression: male liver

Adult OR medaka ~6 months of age were anesthetized by immersion in ice-cold ERM and sacrificed by severing the spinal cord. Livers were dissected individually and snap frozen in liquid nitrogen. RNase ZAP (Sigma) was used throughout all isolations to prevent RNA degradation. Total organ RNA from homogenates was extracted using RNA Bee (Tel-Test) according to the manufacturer's instructions using a Kinematica Polytron homogenizer. Both quality (260/280 ratio) and quantity of resultant RNA samples was determined using a NanoDrop ND-1000 spectrophotometer. RNA was reverse transcribed into cDNA using the high-capacity cDNA master kit (Applied Biosystems) using random hexamer as primer. Relative levels of Fxrα1, Fxrα2, and 18S rRNA were measured using quantitative, realtime PCR (qPCR) in liver. The sequence for 18S ribosomal RNA was identified using the Medaka Genome Browser (DNA Sequencing Center, National Institute of Genetics, Japan) available at http://dolphin.lab.nig.ac.jp/medaka/, and Ensembl (available at http://www.ensembl.org/index.htm). Medaka specific qPCR primers for 18S RNA, Fxrα1, and Fxrα2 were constructed using PrimerQuest (Integrated DNA Technologies) and are listed in Table 1. Relative quantitation of gene expression within each reaction was calculated as described (Fu et al. 2005). Ct values of Fxrα1 and Fxrα2 were subjected to correction by their respective primer efficiencies and corrected values were then normalized to their corresponding 18S RNA values.

Plasmids

A Gal4DBD-FxrαLBD chimera was created by amplifying the medaka FxrαLBD (beginning at GMLAEC…C-terminus) through PCR as described previously, using the following primers containing *Kpn*I and *Bam*HI restriction sites (KpnI-FxrαLBD Fwd and BamHI-FxrαLBD Rev). The resulting PCR product was introduced into the pCR 2.1 vector as previously described, excised using *Kpn*I and *Bam*HI (New England Biolabs, Ipswich, MA), and inserted uni-directionally into the XgalX vector, which contains the translation initiation sequence (amino acids 1–76) of the glucocorticoid receptor fused to the DNA binding domain (amino acids 1–147) of the yeast Gal4 transcription factor in the pSG5 expression vector (Stratagene, La Jolla, CA) (Lehmann et al. 1995). The resulting construct was sequenced to ensure a proper reading frame. The LBD for medaka Fxr is located 3' of the differences between Fxrα1 and α2, thus a single fusion construct represents the LBD for both isoforms since they are 100% identical in this region.

Full-length Fxrα1 was excised from pCR 2.1 using *Eco*RI (New England Biolabs) and introduced into the expression vector pSG5 (Stratagene) using T4 DNA ligase (New England Biolabs). The resulting construct (Fxrα1/pSG5) was transformed, cultured, and isolated as described above. Fxrα2 was excised from pCR 2.1 using *Eco*RI and *Bam*HI and inserted unidirectionally into pSG5 in the same manner. Proper orientation of Fxrα1 and Fxrα2 within the vector was confirmed by PCR screening and sequencing in both directions.

Cell culture

All media and reagents were obtained from Gibco (Carlsbad, CA). PLHC-1 cells were cultured in flasks with plug caps (Corning, Corning, NY) using Leibovitz's L-15 CO_2 Independent Medium (phenol red free) containing heat-inactivated fetal bovine serum (10%) and 100 μg/mL gentamicin. The cells were maintained following standard cell culture protocols in a 29° C incubator, using 1× Trypsin-EDTA for splitting when necessary (~80% confluency). CV-1 cells were cultured in flasks with vented caps (Corning) using Dulbecco's Modified Eagle's Medium containing heat-inactivated fetal bovine serum (10%), glucose (4.5 g/L), L-glutamine, phenol red, HEPES buffer (25 mM), and penicillin-streptomycin (1×). The cells were maintained following standard cell culture protocols in a 37°C/5% CO_2 incubator, using 1× Trypsin-EDTA for splitting when necessary.

HPLC analysis of medaka bile

HPLC analysis of medaka bile was performed as described previously with some modifications (Rossi et al. 1987) using a pooled sample of five gallbladders from STII male medaka dissolved in 150 μL 100% methanol. An octadecylsilane HPLC column (RP C-18) was used, with isocratic elution at 0.75 ml/min. The eluting solution was composed of a mixture of methanol (67.4% by volume) and 0.01 M KH_2PO_4 adjusted to an apparent pH of 5.3. Conjugated BAs were quantified in the column effluent by monitoring the absorbance at 205 nm (for the amide bond). The initial structural assignments were made by comparison with the relative retention time of known standards. Portions of the HPLC effluent were also collected and analyzed by MS to further characterize the HPLC peaks.

MS analysis of medaka bile

STII medaka bile diluted in 100% methanol (as described above) was analyzed by electrospray ionization (ESI) mass spectroscopy using a Perkin-Elmer SCIEX atmospheric pressure instrument API-III (Perkin-Elmer Life and Analytical Sciences, Inc., Boston, Massachusetts) modified with a nano-ESI (Proxeon, Denmark) and operated as previously described (Chatman et al. 1999). Bile alcohol sulfates were detected by operating the instrument in the "parents of 97" mode to observe the loss of sulfate, and BA taurine amidates were detected by operating the instrument in the "parents of 124" mode to observe the loss of taurine.

Transfection and luciferase assays

Agonist screening using the Gal4 system—PLHC-1 cells were seeded in 24-well plates at 2–3 × 10^5 cells/well and transfected at 90–95% confluency using Lipofectamine 2000 (Invitrogen) in serum-free Leibovitz's L-15 Medium as directed by the manufacturer, using the following amounts of plasmid: 15 ng pRL-CMV (*Renilla* luciferase normalizing plasmid, Promega), 0–200 ng pcDNA3.1-f:PGC1α, 250 ng FxrαLBD/XgalX fusion construct, and 250 ng 5XGal4-TATALuc. The transfection media was replaced six hours later with complete L-15 (containing serum and antibiotics). Following an overnight recovery period, the media was replaced with complete L-15 containing one of several BAs (0.1, 1, 10, 50, 100 μM), retinoids (5 μM all-*trans* RA, 5 μM 9-*cis* RA, 10 μM TTNPB), other steroids (100 μM DHT, DHEA, and 17ß-estradiol), or GW4064 (0.1, 1.0, 10 μM) dissolved in DMSO, or DMSO alone to serve as a control (<0.1% total solution). Twenty-four hours post-exposure, the cells were lysed passively according to the protocols described in the Dual Luciferase Reporter Assay System (Promega) and tested for luciferase activities using a DLReady TD-20/20 luminometer (Turner BioSystems, Sunnyvale, CA).

Transactivation assays with full-length Fxrα1 and Fxrα2—Due to the high endogenous FXR activity in PLHC-1 cells, the full-length experiments were performed in CV-1 cells. When confluent in T75 flasks, CV-1 cells were passed as previously noted and grown for at least 72 hours in DMEM/F12 phenol red free media containing 5% charcoal/dextran treated FBS (HyClone), 15 mM HEPES, L-glutamine, and 2 mM glucose. These cells were then used in luciferase experiments. The DMEM/F12 media was also used for dosing the cells following transfection. To confirm the Gal4 results and to demonstrate interaction of Fxrα isoforms with IR-1 response elements, CV-1 cells were seeded in 24-well plates at 1 × 10^5 cells/well and transfected overnight with 15 ng pRL-CMV, 50 ng of either Fxrα1 or Fxrα2/pSG5, 150 ng $(hsp27EcRE)_2$-tk-Luc (containing two imperfect IR-1 response elements) (Forman et al. 1995), and 100 ng pcDNA3.1-f:PGC1α using Lipofectamine (Gibco). The cells were dosed in DMEM/F12 media as previously described for PLHC-1 cells. Twenty-four hours post-exposure the cells were lysed passively, as previously noted, and luciferase activities recorded.

Mammalian two-hybrid screening—CV-1 cells were transfected with 250 ng 5XGal4-TATA-Luc containing binding sites for the yeast Gal4 transcription factor; 75 ng pM.PGC1αL2 or pM.SRC-1 expression vector containing a cofactor nuclear receptor interaction domain fused to the yeast Gal4 DNA-binding domain; 75 ng Fxrα1/pSG5 or Fxrα2/pSG5 and 15 ng pRL-CMV (*Renilla* luciferase) for transfection normalization. Controls consisted of transfections containing empty pM, pSG5 or both empty pM and pSG5 vectors. The cells were dosed in DMEM/F12 media with 1 μM GW4064 or DMSO (<0.1% total solution). The cells were lysed passively 24 hours post-exposure and luciferase activities recorded as previously described to determine receptor-cofactor interactions.

Phylogeny

A phylogenetic tree was constructed via the neighbor-joining method with Poisson correction and bootstrap test using full length FXR α and ß protein sequences (published and predicted) containing receptor AF-1, DBD, hinge, LBD and AF-2 domains. Included in the analysis were FXR sequences from human, mouse, rat, dog, cow, chicken, zebrafish, stickleback, pufferfishes (*Takifugu* and *Tetraodon*), and the little skate. The phylogenetic analysis was performed using MEGA 4 (Kumar et al. 2004).

In silico molecular modeling studies of Fxrα ligand-binding domain

A structural model of Fxrα's LBD was constructed using the MOE-homology model tool, part of the MOE suite (Chemical Computing Group 2007). The published crystal structure of rat FXR in complex with 6α-ethyl-chenodeoxycholic acid (PDB ID = 1OSV) served as the modeling template (Mi et al. 2003). Several energy minimization-based refinement procedures were implemented on the initial model, and the quality of the final model was confirmed by the WHATIF-Check program. Molecular docking studies were performed on CDCA and GW4064 into medaka FXR structural models using the GOLD docking program (Jones et al. 1997). During the docking process, the protein was held fixed while full conformational flexibility was allowed for ligands. For each ligand, 30 independent docking runs were performed to achieve the consensus orientation in the ligand-binding pocket. The ligand-protein interactions were analyzed and represented by a schematic diagram generated using LIGPLOT software (Wallace et al. 1995).

Statistics

All results for dual luciferase assays were expressed as the mean fold induction normalized to control (DMSO) ± SEM. Statistical analyses were performed using Statview 9.0 for Mac (The SAS Institute, Cary, NC). Groups were tested using ANOVA followed by Fisher's PLSD post-hoc test. A p value of < 0.05 was considered significant.

RESULTS

Identification of two medaka FXRα isoforms: Fxrα1 and Fxrα2

Through screening the medaka genome database we detected a single FXRα gene exhibiting a high degree of homology with mouse FXRα used as our BLAST query. This sequence is located on medaka chromosome 6, position 16,621,084–16,632,937 (+ direction). A second Fxrα mRNA transcript, Fxrα2, was identified through 5' rapid amplification of cDNA ends (5' RACE). Further analysis of the medaka genome did not reveal a second Fxrα location, suggesting that the Fxrα1 and α2 are products of alternative splicing of a single gene locus. The protein sequences and alignment of Fxrα1 and Fxrα2 is shown in Figure 1A. Comparisons of genomic and cDNA sequences for both transcripts demonstrated a second translational start site within intron 4 of Fxrα1 as illustrated in Figures 1B and 1C. Exon 1 and the 5' UTR of Fxrα2's open reading frame are found within intron 4 of Fxrα1. This alternate start site results

in the truncation of Fxrα2 by 22 amino acids at the 5' end of the protein. Structurally, Fxrα1 consists of 11 exons total, while Fxrα2 consists of nine. Medaka FXRα1's coding region is 1458 bases long (485 amino acids + stop codon) and Fxrα2's coding region is 1392 bases long (463 amino acids + stop codon). The 5' UTR for Fxrα1 and Fxrα2 have different lengths (99 bp and 264 bp respectively), which may contribute to tissue specific expression. Both Fxrα isoforms are significantly expressed in male liver (Figure 1D); expression in other organs is as described in Howarth et al 2010.

Analyses of functional NR protein domains demonstrated that Fxrα1 contains 136 amino acids in the AF1 domain, 66 aa in the DBD, 63 aa in the hinge region, and 220 aa in the LBD/AF2 domain (not shown). The AF1 domain of Fxrα2 contains 114 amino acids; all other domains are the same as in Fxrα1. Both isoforms show high amino acid sequence identity to the FXRα sequences of other species in the DBD and LBD/AF2 regions. The LBD/AF2 for Fxrα exhibits highest similarity to the predicted FXRα for zebrafish (*Danio rerio*) at 80% amino acid sequence identity (Table 2), as determined through ClustalW analyses (SDSC Biology Workbench, URL: http://workbench.sdsc.edu). The FxrαLBD is also highly similar to mammalian/non-mammalian FXRαLBDs (chicken: 73%; mouse: 71%; rat: 70%; human: 70%; dog: 69%). This is also depicted in the phylogenetic analysis shown in Figure 2. Phylogenetic comparisons of full-length medaka Fxrα1 and α2 with additional FXR α and ß sequences from other species (human, dog, cow, rat, mouse, stickleback, little skate, zebrafish, pufferfishes [*Tetraodon* and *Fugu*], chicken) demonstrate a distinct separation between the FXRα and FXRβ genes. Within the FXRα clade, two distinct subclades were formed, separating aquatic and terrestrial species. FXRα sequences are organized in accordance with species classification within the teleost clade. Since the FXRα sequences from *Fugu*, *Tetraodon* and zebrafish were identified through analysis of available genomes (Ensembl), the presence or absence of multiple splice variants for these species has not been determined.

Medaka bile contains C_{24} and C_{27} bile acids

HPLC and nanoESI-MS analyses demonstrated that medaka bile contains both C_{24} and C_{27} BAs as taurine-conjugates (Figure 3 shows the HPLC chromatogram). Medaka bile consists of approximately 50% C_{24} BAs and 50% C_{27} BAs. The structures for two of the three major C^{27} BAs are unknown, as they represent novel compounds for which we have no standards, but the functional groups within each were elucidated through these analyses (38.792 min, tauro-C_{27} BA with one oxo and two hydroxyl groups; 41.907 min, tauro-(25R)-3α,7α,12α-trihydroxy-5β-cholesten-27-oic acid; and 46.885 min, tauro-C_{27} BA with three hydroxyl groups). The major C_{24} BAs found in STII medaka bile were taurocholic acid and taurochenodeoxycholic acid (14.905 and 28.047 min, respectively). The analysis of medaka bile gave us a point from which to begin screening for potential Fxrα agonists.

Ligand screening using a Gal4DBD-FxrαLBD fusion construct

Through the use of a Gal4DBD-FxrαLBD fusion construct, it was found that both primary (CDCA, CA) and secondary (LCA, DCA) C_{24} BAs effectively activate medaka FXRα (Figure 4A). In this system one Gal4 chimeric construct was used, as both Fxrα isoforms have identical LBDs. Addition of unconjugated BAs resulted in a ~4–11 fold induction, as compared to controls (DMSO). Taurine conjugates of the BAs also activate Fxrα in the Gal4 system. In this system, primary C_{24} BAs present in medaka bile activated Fxrα with the following potency: CDCA (4.47 fold) > CA (3.98 fold), while tauro-CDCA and tauro-CA were roughly equal at activating Fxrα (3.15 and 3.23 fold, respectively). The secondary BAs DCA and LCA, formed through 7α-dehydroxylation of CDCA and CA by intestinal flora (Hofmann 1999), activated Fxrα more efficiently in this system: LCA (10.74 fold) > DCA (8.21 fold). The taurine conjugate of LCA also significantly activated Fxrα in this system (10.52 fold). Ursodeoxycholic acid, the 5ß-isomer of CDCA, did not significantly activate the chimeric

construct (1.32 fold). Furthermore, all-*trans* retinoic acid, 9-*cis* retinoic acid, and the synthetic retinoid TTNPB activated Fxrα (Figure 4B) at 1.77 fold, 3.76 fold, and 3.06 fold respectively. Mild activation of skate FXR, a beta isoform, by retinoids has also been recorded (Cai et al. 2007). The sex hormone dihydrotestosterone (DHT) additionally activated Fxrα (2.03 fold), but DHEA did not (Figure 4B). 17ß-estradiol significantly suppressed Fxrα activity compared to DMSO control in this system, (~65% activity compared to controls). Given that both Fxrα isoforms have identical LBDs, it was projected that with the Gal4-LBD fusion construct no difference with *in vitro* transactivation would be observed between the two splice variants.

Enhancement of Gal4DBD-FxrαLBD fusion construct activation through PGC-1α titration

Activation of the FxrαLBD/XgalX fusion construct was enhanced by addition of increasing amounts of human PGC-1α, as seen in Figure 5. Titration of PGC-1α significantly increased the activation of the fusion construct in a dose-responsive fashion when exposed to 1 μM GW4064. Protein sequence alignments of medaka FXRα1 and α2 with mammalian FXRαs (not shown) found that the AF2 domain (helix 12), known to interact with PGC-1α (Savkur et al. 2005), was identical throughout all FXRαs examined.

Transactivation of an IR-1 reporter construct by full-length Fxrα2, but not Fxrα1

To confirm our initial studies in the Gal4 system, we conducted transient transfection assays with full-length Fxrα1 and α2. These studies were performed using a luciferase reporter construct containing two functional, imperfect IR-1 response elements from *Drosophila* hsp27, an ecdysone receptor (EcR) target (Koelle et al. 1991). Mammalian FXRαs as well as *Drosophila* EcR have been shown to bind to IR-1 response elements within the promoters of target genes (Forman et al. 1995). Surprisingly, our results from experiments with full-length constructs of Fxrα1 and α2 showed that only one Fxrα isoform, Fxrα2, responded to agonists and bound to IR-1 response elements (Figure 6A). We were unable to demonstrate Fxrα1's activation by a wide variety of agonists. Fxrα2 was activated by some, but not all, of agonists tested in the Gal4 system including GW4064, CDCA, and DCA. LCA proved to be very toxic to CV-1 cells and thus data could not be reliably collected in this system. Despite both its presence in medaka bile and its activity in the Gal4 system, CA did not activate either Fxrα in our full-length system. Additionally, the main constituent of zebrafish and carp bile, 5α-cyprinol sulfate, did not activate either Fxrα isoform. Following initial agonist screening, dose-responses with CDCA and GW4064 (a synthetic FXR agonist), were performed with Fxrα2/pSG5 and it was noted that Fxrα2 was activated in a dose-responsive fashion by both of these agonists with an EC_{50} of ~40 μM and 9.78 nM, respectively (Figures 6B and C). To ensure that both Fxrα1 and Fxrα2 were expressed in our transfection system, both RNA and protein from CV-1 cells were collected and analyzed by either RT-PCR or western blot (supplemental data figures 1 and 2). Using RT-PCR were able to demonstrate expression of both Fxrα1 and Fxrα2 message indicating successful tranfection and expression of both pSG5Fxrα constructs. RNA isolation was conducted as described in materials and methods followed by an on column DNA digestion to ensure PCR results were from amplification of cDNA and not residual plasmid. Transfection of FLAG-tagged pCMVFxrα constructs were used to ensure appropriate translation of FXR constructs/mRNA in to protein. Western blot analysis using anti-FLAG antibodies demonstrates production of both Fxrα1 and Fxrα2 protein following transient transfection into CV-1 cells.

Mammalian two-hybrid screening shows interaction of Fxrα2 with PGC-1α and SRC-1

To confirm our studies with the Gal4 system, which showed enhancement of activation by addition of PGC-1α, mammalian two-hybrid assays were performed. These studies are key to studying receptor-coactivator interactions; significant transactivation of the reporter by Fxrα cannot occur in this system without the addition of a Gal4-coactivator construct, since the

reporter construct contains Gal4REs. As shown in Figure 7, Fxrα1 and Fxrα2 again are differentially activated *in vitro.* Despite having identical ligand-binding domains, only Fxrα2 interacted with PGC-1α and SRC-1. No significant interaction of Fxrα1 with either coactivator was demonstrated in these assays. Interestingly, interaction between SRC-1 and Fxrα2 was greater than that of PGC-1α, despite previous reports with mammalian FXRs (Kanaya et al. 2004;Savkur et al. 2005).

In silico molecular modeling demonstrates binding of GW4064 and CDCA within the Fxrα ligand-binding domain

A homology model of Fxrα's LBD was constructed using rat FXR as the template. Using this homology model, docking studies were performed with GW4064 (synthetic FXR agonist) and CDCA (Figures 8A and B). The predicted conformation of GW4064 was similar to the recent published crystal structure of human FXR bound with the same compound (Akwabi-Ameyaw et al. 2008). In the medaka FXR model, GW4064 forms a strong electrostatic interaction with the conserved Arg^{344} residue on helix 5 (amino acid numbers correspond to Fxrα1), which mimics the interaction between this Arg residue and the carboxyl group of bile salts, an interaction that plays an important role in recognition of BAs by FXR (Mi et al. 2003). Extensive hydrophobic contacts with the protein, as shown in Figure 8A, contribute to the potent activity of GW4064. Van der Waals interactions with Leu^{478} and Trp^{482} may stabilize helix 12 into an active conformation for receptor activation.

Docking studies predicted that CDCA was bound to FxrαLBD in an upside down manner in comparison with the observed orientation of 6α-ethyl-CDCA in rat FXR (Figure 8B) (Mi et al. 2003). Further validation would be needed to confirm if this is a biological relevant orientation for CDCA in Fxrα. In addition to the charged interactions with Arg^{344}, the 7α-hydroxy group hydrogen bonded with its backbone carbonyl oxygen. This interaction would be lost for BAs such as UDCA, which have a 7β-hydroxy group. This interpretation is consistent with the functional data that shows no activation of Fxrα by UDCA. Compared with GW4064, less hydrophobic contacts were present for CDCA, which is consistent with its lower potency relative to GW4064 in functional assays of Fxrα.

DISCUSSION

The function of FXRα as a BA sensor has been well characterized in mammalian systems. However, little is known about the teleost biliary system from both structural and molecular perspectives. Our laboratory has recently published an in-depth structural assessment of the medaka biliary tree (Hardman et al. 2007), but little is known about BA-nuclear receptor (NR) signaling in teleosts. This paper is a stepping-stone that furthers our understanding of BA homeostasis within this model organism.

The generation of genomic databases for an array of organisms has greatly facilitated and expanded the data mining process. These advances have allowed researchers to locate orthologous genes within the genome of interest through the use of well-studied sequences from phylogenetically distant species. In humans, four isoforms of FXRα exist, differing in both the presence or absence of a four amino acid insert (MYTG) within the hinge region, and in the length of the AF1 region (Huber et al. 2002). The absence of the MYTG insert within the hinge region of both Fxrα isoforms suggested that Fxrα1 and Fxrα2 are similar to the α4 or α2 isoforms of human FXRα, respectively. Of importance is the presence of a histidine and tryptophan within the FxrαLBD ($His^{460,438}$ and $Trp^{482,460}$ of Fxrα1 and α2, respectively) in the same location as mammalian FXRαs (His^{444} and Trp^{466} for rat FXRα). These amino acids play a crucial structural role by stabilizing the active conformation of FXRα in the presence of an agonist (Mi et al. 2003). The His-Trp “switch” is present in all FXRα sequences used for phylogenetic analyses. Fxrα1 and α2 clustered with predicted sequences for several teleosts

(zebrafish, pufferfishes, and stickleback), while the mammalian sequences clustered separately. Furthermore, all FXRß sequences formed a distinct cluster separate from FXRα sequences, which further separate into mammalian and piscine clades. The skate FXRß fell within the teleost FXRα clade, but is an outlier within this group.

To give a starting point for Fxrα agonist screening, HPLC and MS analyses of medaka bile were performed. BAs are derived from cholesterol through a complex series of steps involving multiple cytochrome P450s and other enzymes (Russell 2003). Cholesterol is used by vertebrates for maintenance of membrane fluidity, neurotransmission, reproduction, bone formation, and solubilization of fats. In the metabolic turnover of cholesterol, it must be converted into water soluble products suitable for excretion. As a result, bile salts and steroid hormones have evolved as important signaling molecules over the course of time. Nematodes such as *C. elegans* utilize dafachronic acids and 3-keto BA-like steroids for dauer pathway signaling (Gerisch et al. 2007). Early vertebrates such as the little skate (*Leucoraja erinacea*) metabolize cholesterol into C_{27} sulfated polyhydroxylated bile alcohols such as scymnol sulfate (Karlaganis et al. 1989). Cyprinid fish also generate C_{27} sulfated bile alcohols from cholesterol, predominantly 5α-cyprinol sulfate (Goto et al. 2003). Modern vertebrate species such as mammals have evolved the ability to convert C_{27} bile alcohol sulfates and BAs into C_{24} acids that are capable of undergoing an enterohepatic circulation. A number of different vertebrate groups have converged on C_{24} BA synthesis through independent pathways; some species within these groups are transitional species capable of synthesizing both C_{27} and C_{24} BAs (Hofmann et al., 2009). The medaka is an example of a species in transition, as its bile contains both C_{27} and C_{24} acids in approximately equal amounts. While the structures of most of the C_{27} acids are unknown, the predominant C_{24} acids present in medaka bile are taurocholic and taurochenodeoxycholic acids.

By creating a Gal4DBD-FxrαLBD fusion construct, we were able to locate efficient Fxrα agonists without knowing its DNA-binding properties. Both primary (CDCA, CA) and secondary (LCA, DCA) BAs were able to activate the fusion construct. Other steroids and retinoids were also able to activate this system. Activation of the medaka Fxr construct by retenoids may be due to the permissive nature of the FXR:RXR heterodimer where either of the heterodimeric partners can bind their cognate ligands and induce transactivation (Forman et al., 1995). However in another study the RXR agonist LG100268 was shown to antagonize the induction of BSEP expression mediated by FXR ligands CDCA and GW4064. In this instance authors suggest that FXR/RXR is a conditionally permissive heterodimer resulting in both a decrease in binding of FXR/RXR heterodimer to the BSEP-FXRE and reduced ability to recruit coactivators to FXR/RXR (Kassam et al, 2003). However, under our conditions with use of the Gal4 system, we demonstrate enhanced activation of Fxrα by addition of the nuclear receptor coactivator PGC-1α in a dose-responsive fashion.

Once agonists were located for Fxrα using the Gal4 system, full-length transactivation properties using both Fxrα isoforms were elucidated. Here we show that Fxrα2 interacted with IR-1 response elements in the presence of an agonist whereas Fxrα1 did not, despite having identical ligand-binding domains. Given that both Fxrα forms are expressed and translated in our transient transfection system, differences *in vitro* activity may point to selective ligand-specific responses *in vivo* in which each Fxrα isoform mediates activation of distinct gene targets in the same or different tissues within the organism. It may also demonstrate the importance of the AF1 domain to overall receptor function, ligand fidelity, and ability to bind differential response elements within the promoters of target genes. This idea is supported by the surprising finding that CA activated Fxrα in the Gal4 system, but did not activate either isoform in the full-length studies. Furthermore, neither Fxrα isoform was activated by the major constituent of zebrafish bile, 5α-cyprinol sulfate. This data, in correlation with HPLC analyses of medaka bile, show medaka as an evolutionary “species in transition” that falls between

cyprinid fishes that synthesize C_{27} bile alcohols and mammals that generate C_{24} acids. Since these isoforms are the result of alternative splicing, their differences in activity are not the result of sub- or neofunctionalization, as would be predicted with gene paralogs that arose as the result of a whole genome duplication event in the evolution of teleost fish (Taylor et al. 2001; Chen et al. 2004; Christoffels et al. 2004) and is observed with medaka VDRα and ß (Howarth et al. 2008). We additionally tested the idea that Fxrα1 may act as a dominant negative Fxrα form, silencing the activity of Fxrα2 through competition for an IR1 response element. This hypothesis is based on the fact that Fxrα1 is more abundant in medaka liver than Fxrα2. Studies were thus conducted where a fixed concentration of Fxrα2 was co-transfected into CV-1 cells with increasing amounts (up to 4×) of Fxrα1. Results of this experiment however did not produce significant suppression of Fxrα2 transactivation even at higher concentrations of Fxrα 1 (supplementary data figure 3) indicating that Fxrα1 is likely not playing a suppressive role under these conditions.

Here we demonstrate that nuclear receptor biology in teleosts is an area in which we anticipate that novel receptor functions may be discovered. Furthermore, the synthetic FXRα agonist GW4064 (Maloney et al. 2000) was found to induce α2 activation more efficiently than commercially available C_{24} BAs and in a dose-responsive fashion. This is a significant finding, as GW4064 is specific to this receptor and is widely used as a chemical tool in mammalian systems to elicit a specific FXRα-mediated response. As shown here, it can also be used to definitively demonstrate conservation in gene function between mammalian and teleost FXRα orthologs.

In silico molecular modeling studies with FxrαLBD supported our findings of a differential potency between GW4064 and CDCA, by demonstrating increased hydrophobic contacts between Fxrα and GW4064 versus with CDCA. While GW4064 has eleven expected hydrophobic contacts within the ligand-binding pocket of the FxrαLBD, CDCA only has seven. Furthermore, modeling studies indicate an “upside-down” orientation of CDCA in the ligand-binding pocket of Fxrα in comparison to rat FXR (Mi et al. 2003), due to the charged interactions with Arg^{344} and hydrogen-bonding of the 7α-hydroxy group of CDCA with a carbonyl oxygen in the protein backbone. This H-bonding is lost with 7ß-hydroxy BAs such as UDCA, which falls out of plane, thus implying that UDCA would not be a good Fxrα agonist. Our mammalian two-hybrid studies suggest that Fxrα activation by CDCA does not result in significant interaction with the NR coactivator PGC-1α for either isoform (data not shown) despite both our data that demonstrated CDCA's ability to activate Fxrα2 in a dose-responsive fashion, and reports from the mammalian literature (Kanaya et al. 2004; Savkur et al. 2005). Taken together, these data suggest that the upside-down orientation of CDCA within the ligand-binding pocket may play a role in NR-coregulator interaction by stabilizing the LBD in a different conformation, but this has not been investigated to date. Conversely, interaction of FxrαLBD with PGC-1α and GW4064 was demonstrated through enhanced transactivation with coregulator addition in the Gal4 system and through mammalian two-hybrid assays with Fxrα2. This data suggests a strong conservation of protein-protein interactions and molecular function of FXRα from distantly related species. Fxrα2 additionally demonstrated significant interaction with the nuclear receptor coactivator SRC-1, while Fxrα1 showed no significant interaction with either PGC-1α or SRC-1. These findings show the importance of the AF1 domain in protein-protein interactions between medaka NRs and coactivators/corepressors. One key to our understanding of Fxrα function *in vivo* and *in vitro* will be the isolation of medaka C_{27} BAs and an assessment of differential activities between Fxrα1 and α2 with these ligands. As Fxrα1 and α2 exhibit differential activations, activity with differential ligands may be a means to diversify nuclear receptor signaling *in vivo*. However, it is pertinent to note that human SRC-1 and PGC-1α were used in our mammalian two hybrid assays. Therefore, it is possible that medaka Fxrα1 is unable to interact with human co-activators while medaka Fxrα2 is more promiscuous. Further research involving medaka SRC-1 and PGC-1α is needed

to further elucidate the function of Fxrα1, particularly given its significant expression in the adult liver.

While mammalian NRs have been widely studied through both *in vitro* and *in vivo* techniques, little information is known about the majority of NRs in aquatic model organisms. Our data demonstrates conservation of function between mammalian and medaka FXRα at the *in vitro* level by showing similar ligand and DNA binding properties and NR-coactivator interactions. The differential activities of Fxrα1 and α2 *in vitro* may point to differential expression and gene activation *in vivo*. For example, the four human isoforms of FXRα, which have different 5' UTR and AF1 domains, are differentially expressed within the liver, intestine, kidney, and adrenal glands (Huber et al. 2002). The information presented here, in conjunction with recent data published by our laboratory elucidating the structure of the medaka biliary tree (Hardman et al. 2007), further enhances our ability to use this unique organism as a model for in-depth, high-throughput liver toxicity studies.

Supplementary Material

Refer to Web version on PubMed Central for supplementary material.

Acknowledgments

We thank Dr. Donald McDonnell for 5XGal4-TATA-Luc, Dr. Bruce Spiegelman for pcDNA3.1-f:PGC1α, Dr. Patrick Casey for use of his DLReady TD 20/20 luminometer, Dr. Rich Di Giulio for PLHC-1 cells, Linda Moore for CV-1 cells, and Dr. Steven Kliewer for GW4064. This work was supported in part by the National Center for Research Resources (RO1 RR018583-02 to DEH and SWK), National Cancer Institute (R21CA105084-01A1 to SWK and DEH), Duke University Integrated Toxicology and Environmental Health Program, and by an EPA STAR Graduate Fellowship awarded to DLH (FP916427).

REFERENCES

Akwabi-Ameyaw A, Bass JY, et al. Conformationally constrained farnesoid X receptor (FXR) agonists: Naphthoic acid-based analogs of GW 4064. Bioorg Med Chem Lett 2008;18(15):4339–43. [PubMed: 18621523]

Bertrand S, Thisse B, et al. Unexpected Novel Relational Links Uncovered by Extensive Developmental Profiling of Nuclear Receptor Expression. PLoS Genet 2007;3(11):e188. [PubMed: 17997606]

Braunbeck TA, Teh SJ, et al. Ultrastructural alterations in liver of medaka (Oryzias latipes) exposed to diethylnitrosamine. Toxicol Pathol 1992;20(2):179–96. [PubMed: 1475579]

Cai SY, Xiong L, et al. The farnesoid X receptor, FXR{alpha}/NR1H4, acquired ligand specificity for bile salts late in vertebrate evolution. Am J Physiol Regul Integr Comp Physiol 2007;293(3):R1400–9. [PubMed: 17567710]

Chatman K, Hollenbeck T, et al. Nanoelectrospray mass spectrometry and precursor ion monitoring for quantitative steroid analysis and attomole sensitivity. Anal Chem 1999;71(13):2358–63. [PubMed: 10405603]

Chemical Computing Group, I. Molecular Operating Environment. Montreal, Quebec, Canada: 2007.

Chen WJ, Orti G, et al. Novel evolutionary relationship among four fish model systems. Trends Genet 2004;20(9):424–31. [PubMed: 15313551]

Christoffels A, Koh EG, et al. Fugu genome analysis provides evidence for a whole-genome duplication early during the evolution of ray-finned fishes. Mol Biol Evol 2004;21(6):1146–51. [PubMed: 15014147]

Denson LA, Sturm E, et al. The orphan nuclear receptor, shp, mediates bile acid-induced inhibition of the rat bile acid transporter, ntcp. Gastroenterology 2001;121(1):140–7. [PubMed: 11438503]

Edwards PA, Kast HR, et al. BAREing it all: the adoption of LXR and FXR and their roles in lipid homeostasis. J Lipid Res 2002;43(1):2–12. [PubMed: 11792716]

Forman BM, Goode E, et al. Identification of a nuclear receptor that is activated by farnesol metabolites. Cell 1995;81(5):687–93. [PubMed: 7774010]

Fu M, Sun T, et al. A Nuclear Receptor Atlas: 3T3-L1 adipogenesis. Mol Endocrinol 2005;19(10):2437–50. [PubMed: 16051663]

Gerisch B, Rottiers V, et al. A bile acid-like steroid modulates Caenorhabditis elegans lifespan through nuclear receptor signaling. Proc Natl Acad Sci U S A 2007;104(12):5014–9. [PubMed: 17360327]

Germain P, Staels B, et al. Overview of nomenclature of nuclear receptors. Pharmacol Rev 2006;58(4): 685–704. Pharmacol Rev **58**(4): 685-704. [PubMed: 17132848]

Goodwin B, Jones SA, et al. A regulatory cascade of the nuclear receptors FXR, SHP-1, and LRH-1 represses bile acid biosynthesis. Mol Cell 2000;6(3):517–26. [PubMed: 11030332]

Goto T, Holzinger F, et al. Physicochemical and physiological properties of 5alpha-cyprinol sulfate, the toxic bile salt of cyprinid fish. J Lipid Res 2003;44;(9):1643–51. [PubMed: 12810826]

Hardman RC, Volz DC, et al. An in vivo Look at Vertebrate Liver Architecture: Three-Dimensional Reconstructions from Medaka (Oryzias latipes). Anat Rec (Hoboken) 2007;290(7):770–82. [PubMed: 17516461]

Hofmann AF. The continuing importance of bile acids in liver and intestinal disease. Arch Intern Med 1999;159(22):2647–58. [PubMed: 10597755]

Howarth DL, Law SH, et al. Paralogous vitamin D receptors in teleosts: transition of nuclear receptor function. Endocrinology 2008;149(5):2411–22. [PubMed: 18258682]

Howarth DL, Law SH, et al. Exposure to the synthetic FXR agonist GW4064 causes alterations in gene expression and sublethal hepatotoxicity in eleutheroembryo medaka (Oryzias latipes). Toxicol Appl Pharmacol 2010;243(1):111–121. [PubMed: 19963001]

Huber RM, Murphy K, et al. Gene 2002;Generation of multiple farnesoid-X-receptor isoforms through the use of alternative promoters;290(1-2):35–43. [PubMed: 12062799]

Jones G, Willett P, et al. Development and validation of a genetic algorithm for flexible docking. Journal of Molecular Biology 1997;267(3):727–748. [PubMed: 9126849]

Kanaya E, Shiraki T, et al. The nuclear bile acid receptor FXR is activated by PGC-1alpha in a ligand-dependent manner. Biochem J 2004;382(Pt 3):913–21. [PubMed: 15202934]

Karlaganis G, Bradley SE, et al. A bile alcohol sulfate as a major component in the bile of the small skate (Raja erinacea). J Lipid Res 1989;30(3):317–22. [PubMed: 2723539]

Koelle MR, Talbot WS, et al. The Drosophila EcR gene encodes an ecdysone receptor, a new member of the steroid receptor superfamily. Cell 1991;67(1):59–77. [PubMed: 1913820]

Kumar S, Tamura K, et al. MEGA3: Integrated software for Molecular Evolutionary Genetics Analysis and sequence alignment. Brief Bioinform 2004;5(2):150–63. [PubMed: 15260895]

Lehmann JM, Moore LB, et al. An antidiabetic thiazolidinedione is a high affinity ligand for peroxisome proliferator-activated receptor gamma (PPAR gamma). J Biol Chem 1995;270(22):12953–6. [PubMed: 7768881]

Liu Y, Binz J, et al. Hepatoprotection by the farnesoid X receptor agonist GW4064 in rat models of intra- and extrahepatic cholestasis. J Clin Invest 2003;112(11):1678–87. [PubMed: 14623915]

Liu Z, Kullman SW, et al. ras oncogene mutations in diethylnitrosamine-induced hepatic tumors in medaka (Oryzias latipes), a teleost fish. Mutat Res 2003;539(1-2):43–53. [PubMed: 12948813]

Lu TT, Makishima M, et al. Molecular basis for feedback regulation of bile acid synthesis by nuclear receptors. Mol Cell 2000;6(3):507–15. [PubMed: 11030331]

Maglich JM, Caravella JA, et al. The first completed genome sequence from a teleost fish (Fugu rubripes) adds significant diversity to the nuclear receptor superfamily. Nucleic Acids Res 2003;31(14):4051–8. [PubMed: 12853622]

Makishima M, Okamoto AY, et al. Identification of a nuclear receptor for bile acids. Science 1999;284 (5418):1362–5. [PubMed: 10334992]

Maloney PR, Parks DJ, et al. Identification of a chemical tool for the orphan nuclear receptor FXR. J Med Chem 2000;43(16):2971–4. [PubMed: 10956205]

Metpally RP, Vigneshwar R, et al. Genome inventory and analysis of nuclear hormone receptors in Tetraodon nigroviridis. J Biosci 2007;32(1):43–50. [PubMed: 17426379]

Mi LZ, Devarakonda S, et al. Structural basis for bile acid binding and activation of the nuclear receptor FXR. Mol Cell 2003;11(4):1093–100. [PubMed: 12718893]

Okihiro MS, Hinton DE. Progression of hepatic neoplasia in medaka (Oryzias latipes) exposed to diethylnitrosamine. Carcinogenesis 1999;20(6):933–40. [PubMed: 10357770]

Otte K, Kranz H, et al. Identification of farnesoid X receptor beta as a novel mammalian nuclear receptor sensing lanosterol. Mol Cell Biol 2003;23(3):864–72. [PubMed: 12529392]

Parks DJ, Blanchard SG, et al. Bile acids: natural ligands for an orphan nuclear receptor. Science 1999;284 (5418):1365–8. [PubMed: 10334993]

Plass JR, Mol O, et al. Farnesoid X receptor and bile salts are involved in transcriptional regulation of the gene encoding the human bile salt export pump. Hepatology 2002;35(3):589–96. [PubMed: 11870371]

Reschly EJ, Ai N, et al. Evolution of the bile salt nuclear receptor FXR in vertebrates. J Lipid Res 2008;49 (7):1577–87. [PubMed: 18362391]

Rossi SS, Converse JL, et al. High pressure liquid chromatographic analysis of conjugated bile acids in human bile: simultaneous resolution of sulfated and unsulfated lithocholyl amidates and the common conjugated bile acids. J Lipid Res 1987;28(5):589–95. [PubMed: 3598401]

Russell DW. The enzymes, regulation, and genetics of bile acid synthesis. Annu Rev Biochem 2003;72:137–74. [PubMed: 12543708]

Savkur RS, Thomas JS, et al. Ligand-dependent coactivation of the human bile acid receptor FXR by the peroxisome proliferator-activated receptor gamma coactivator-1alpha. J Pharmacol Exp Ther 2005;312(1):170–8. [PubMed: 15329387]

Taylor JS, Van de Peer Y, et al. Comparative genomics provides evidence for an ancient genome duplication event in fish. Philos Trans R Soc Lond B Biol Sci 2001;356(1414):1661–79. [PubMed: 11604130]

Volz DC, Bencic DC, et al. 2,3,7,8-Tetrachlorodibenzo-p-dioxin (TCDD) induces organ- specific differential gene expression in male Japanese medaka (Oryzias latipes). Toxicol Sci 2005;85(1):572–84. [PubMed: 15703262]

Wakamatsu Y, Pristyazhnyuk S, et al. The see-through medaka: a fish model that is transparent throughout life. Proc Natl Acad Sci U S A 2001;98(18):10046–50. [PubMed: 11526229]

Wallace AC, Laskowski RA, et al. LIGPLOT: a program to generate schematic diagrams of protein-ligand interactions. Protein Eng 1995;8(2):127–34. [PubMed: 7630882]

Wang H, Chen J, et al. Endogenous bile acids are ligands for the nuclear receptor FXR/BAR. Mol Cell 1999;3(5):543–53. [PubMed: 10360171]

Zollner G, Fickert P, et al. Role of nuclear bile acid receptor, FXR, in adaptive ABC transporter regulation by cholic and ursodeoxycholic acid in mouse liver, kidney and intestine. J Hepatol 2003;39(4):480–8. [PubMed: 12971955]

A

```
FXRa1   MNEWVGPDITVVGPLQIPPSDDFSMSEGAHFFDILGDQGSPLLQDSDILP
FXRa2                          MALVQMQSSRDILGDQGSPLLQDSDILP

FXRa1   FNNYPSMQYPSMEPAMSSTPFYSTQNYYPQYSGDEWYSHTGIYELRKAPL
FXRa2   FNNYPSMQYPSMEPAMSSTPFYSTQNYYPQYSGDEWYSHTGIYELRKAPL

FXRa1   EGSYEGDMKEMSCNVPTVCKKSRHMMQAGRVKGEELCVVCGDKASGYHYN
FXRa2   EGSYEGDMKEMSCNVPTVCKKSRHMMQAGRVKGEELCVVCGDKASGYHYN

FXRa1   ALTCEGCKGFFRRSITKNAVYKCKSGGNCEMDMYMRRKCQECRLRKCKEM
FXRa2   ALTCEGCKGFFRRSITKNAVYKCKSGGNCEMDMYMRRKCQECRLRKCKEM

FXRa1   GMLAECLLTEIQCKSKRLRKNTKTSPGRSTGDETEGADSGDSKQVTSTTK
FXRa2   GMLAECLLTEIQCKSKRLRKNTKTSPGRSTGDETEGADSGDSKQVTSTTK

FXRa1   VPKEKVEITKDQQSLIRLIVDAYNRHQIPQDVTKKLLQEQYSTEENFLLL
FXRa2   VPKEKVEITKDQQSLIRLIVDAYNRHQIPQDVTKKLLQEQYSTEENFLLL

FXRa1   TEIATSQVQVLVEFTKNIPGFLSLDHEDQIALLKGSAVEAMFLRSAQVFS
FXRa2   TEIATSQVQVLVEFTKNIPGFLSLDHEDQIALLKGSAVEAMFLRSAQVFS

FXRa1   RKMPSGHTDVLEERIRKSGISEEFITPLFNFYKSVGELHMVLEEQALLTA
FXRa2   RKMPSGHTDVLEERIRKSGISEEFITPLFNFYKSVGELHMVLEEQALLTA

FXRa1   VTILTPDRPYVKNQQAVERLQEPMVDVLRKLCALKRPQEPQYFARLLGRL
FXRa2   VTILTPDRPYVKNQQAVERLQEPMVDVLRKLCALKRPQEPQYFARLLGRL

FXRa1   TELRTLNHYHAEMLTSWRVNDHKFTPLLCEIWDVQ
FXRa2   TELRTLNHYHAEMLTSWRVNDHKFTPLLCEIWDVQ
```

B

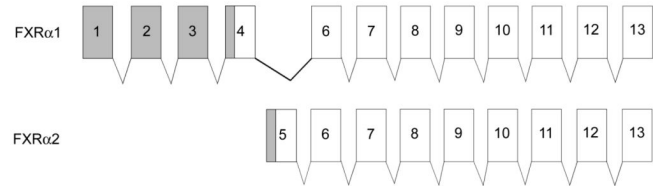

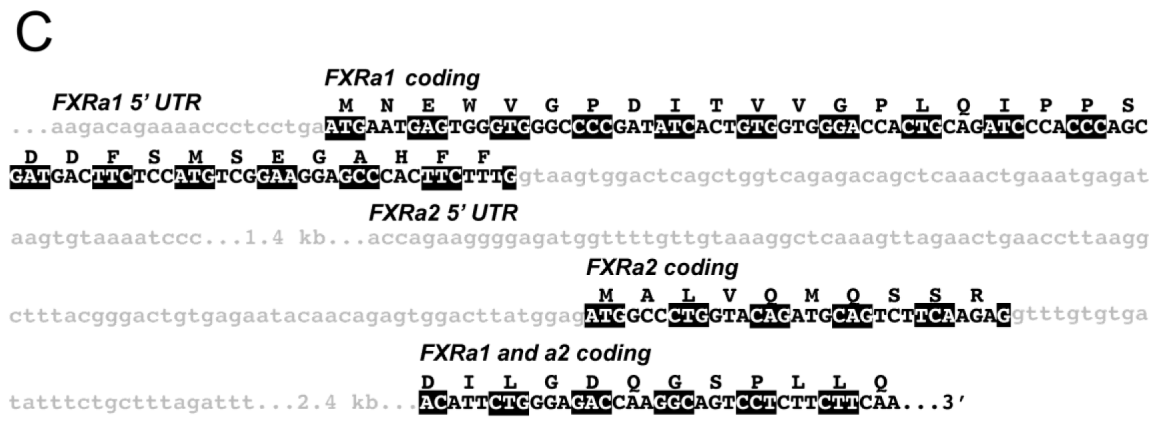

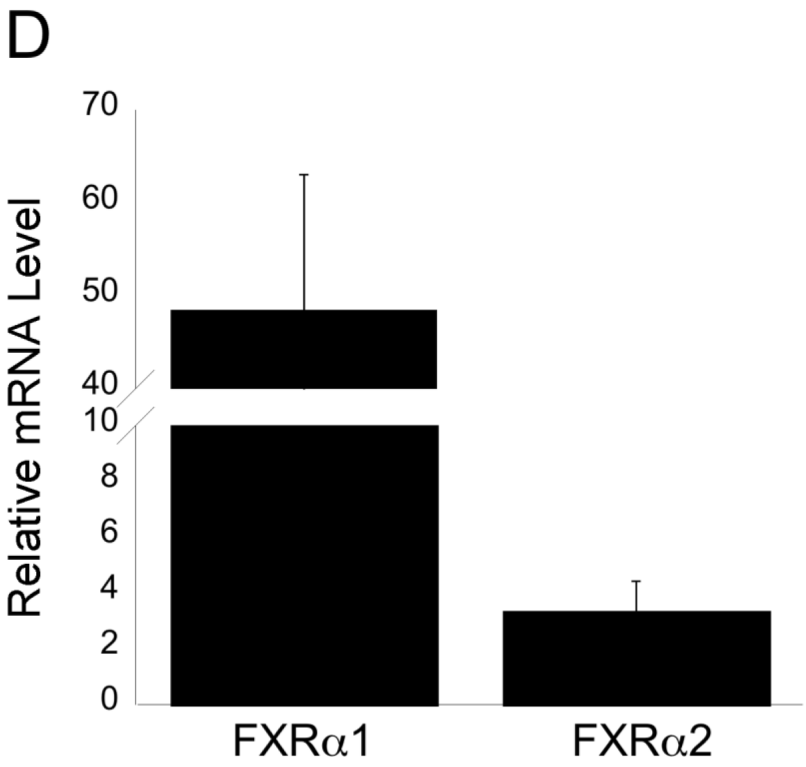

Figure 1. A: Protein sequences of medaka FXRα1 and FXRα2

A gray box denotes the differences between the two isoforms as a result of alternative splicing. B: Fxrα1 and Fxrα2 have different 5' ends due to alternative splicing. As shown here, differential splicing results in the formation of these two isoforms. Gray shading indicates the 5'UTR for each gene. No shading indicates their coding regions. Exons with the same number indicate those that are identical in both Fxrα isoforms. C: Further details on splicing differences between Fxrα isoforms. Light gray shaded, lower case letters indicates noncoding regions. Coding regions for each isoform are specifically marked and denoted in upper case letters. Codons are highlighted alternatively in black and white for clarity. Fxrα2's start codon is

downstream of Fxrα1's and is located in a predicted (Ensembl) Fxrα1 intron. D: Relative Fxrα1 and Fxrα2 levels in male liver. N=5, normalized to 18S RNA levels.

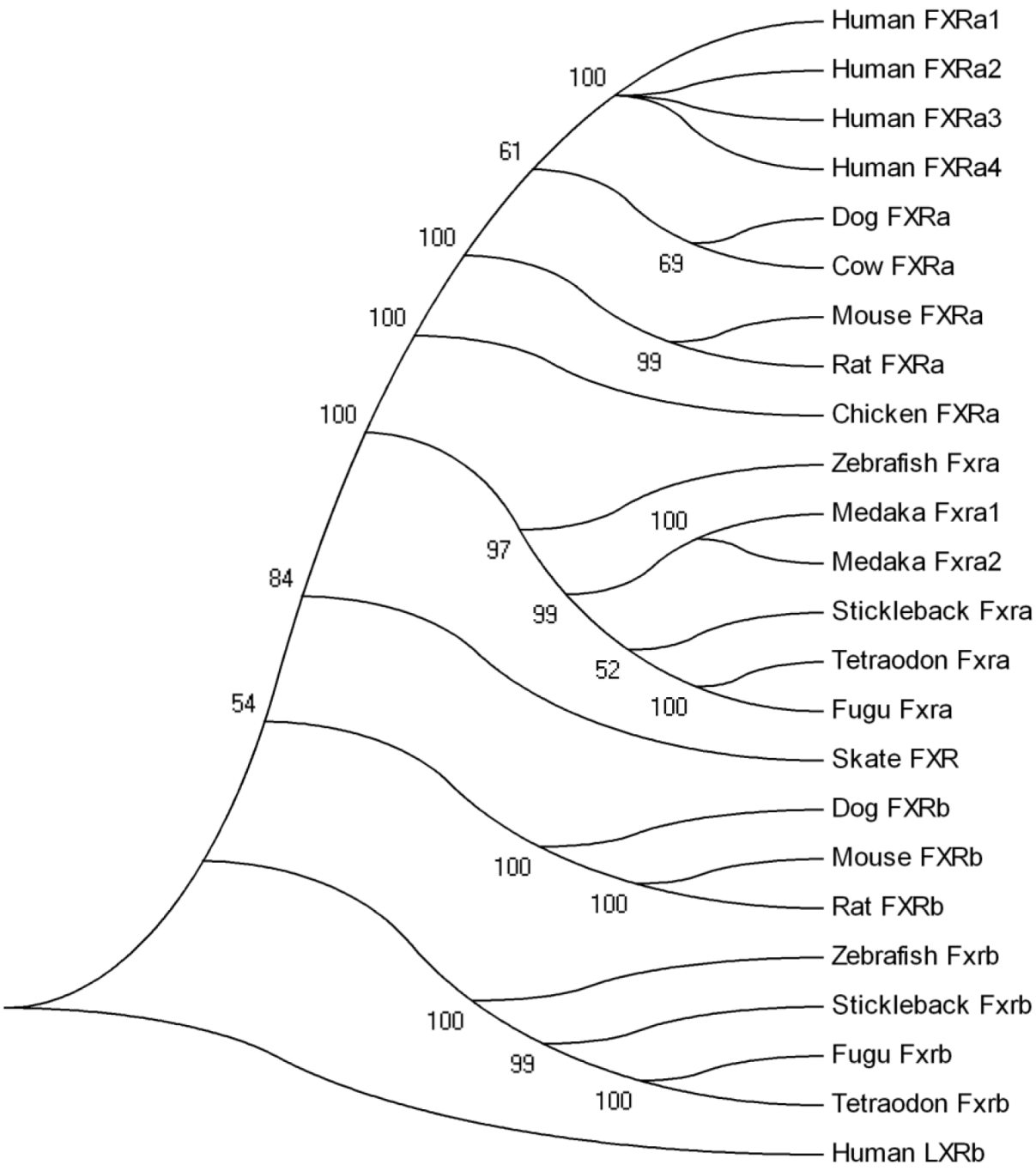

Figure 2. Phylogenetic analysis of FXR alpha and betas

A phylogenetic tree was generated using protein sequences of multiple FXRs using MEGA 4 (Kumar et al. 2004) using a bootstrap tested, neighbor-joining method with Poisson correction.

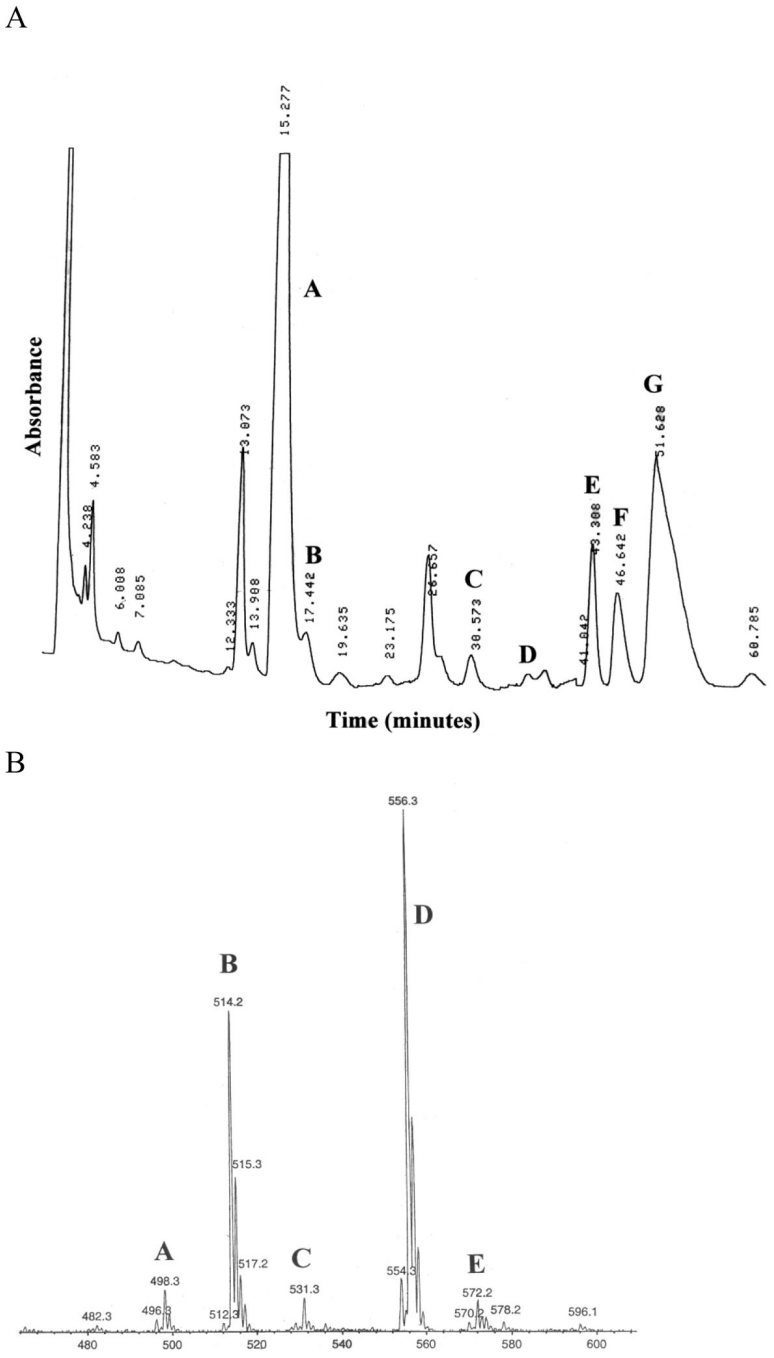

Figure 3. HPLC and MS analyses of medaka bile

Analysis was performed as described in the Methods section of this paper. Major constituents are labeled in HPLC chromatogram as follows: (A) taurocholic acid; (B) tauroallocholic acid; (C) taurochenodeoxycholic acid; (D) taurodeoxycholic acid; (E) unknown taurine conjugated C_{27} bile acid; (F) taurine conjugated 25R-3α,7α,12α-trihydroxy-5β-cholestan-27-oic acid; and (G) unknown taurine conjugated C_{27} trihydroxy bile acid. Major constituents in the MS spectra are labeled as follows: (A) taurine conjugated C_{24} dihydroxy bile acid; (B) taurine conjugated C_{24} trihydroxy bile acid; (C) C_{27} pentahydroxy bile alcohol sulfate; (D) taurine conjugated C_{27} trihydroxy bile acid; and (E) taurine conjugated C_{27} tetrahydroxy bile acid.

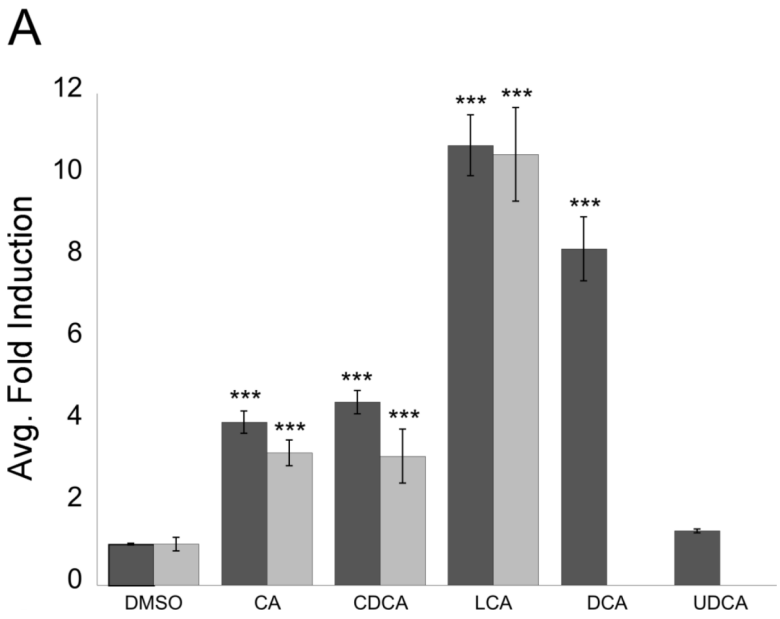

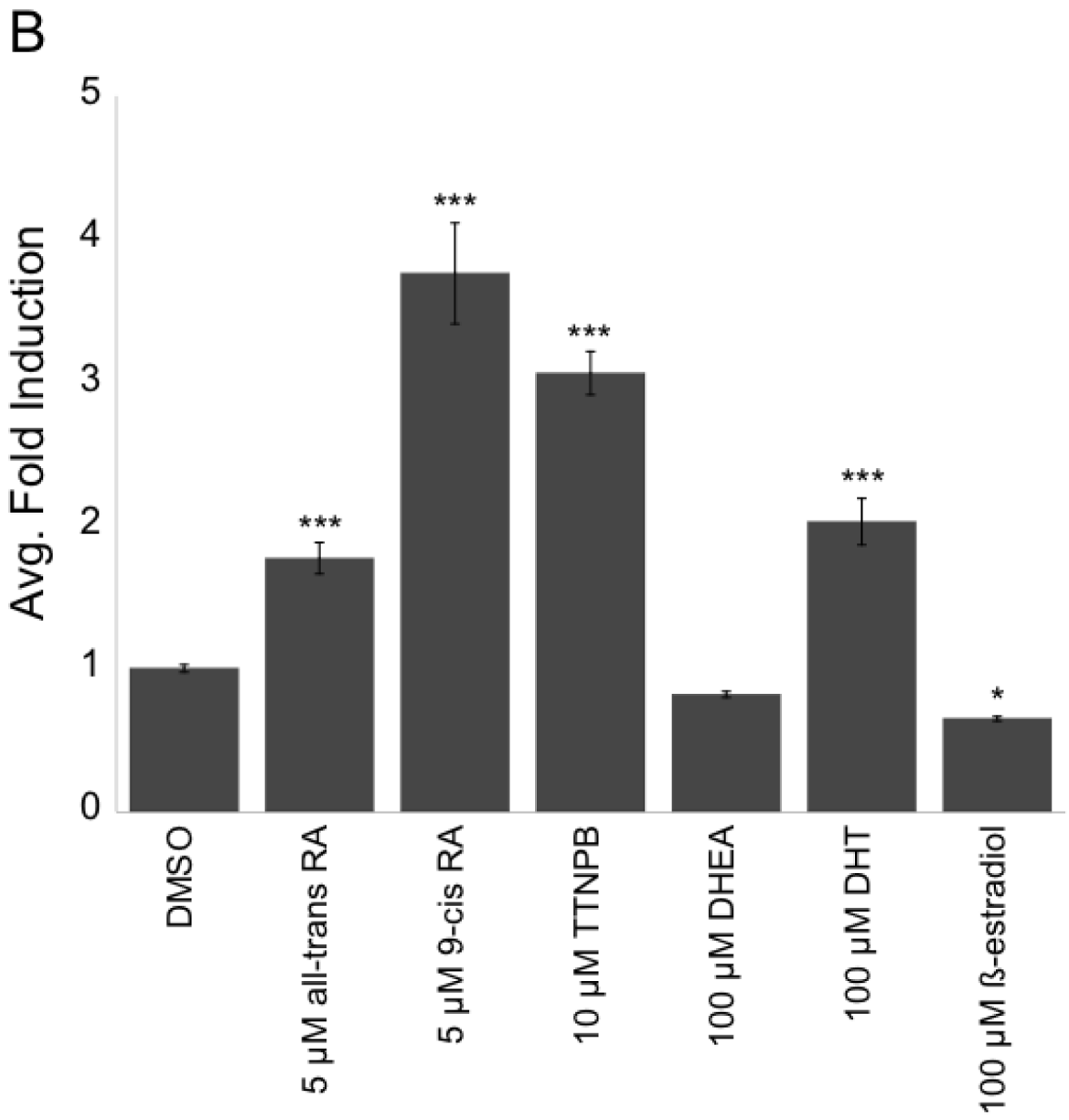

Figure 4. Ligand screen using FxrαLBD/XgalX

Gal4 system was employed to screen for Fxrα agonists. PLHC-1 cells were seeded in 24-well plates at 2–3 × 10^5 cells/well and transfected with pRL-CMV (normalizing plasmid), pcDNA3.1–f:PGC1α (nuclear receptor coactivator), 5XGal4-TATA-Luc (reporter plasmid), and FxrαLBD/XgalX. A: Cells were dosed with 100 µM unconjugated (dark gray bars) or taurine-conjugated (light gray bars) BAs in media for 24 hours. Activation of Fxrα was measured as an average fold induction relative to control (DMSO). Asterisks indicate a statistically significant difference between control and treatment ($p<0.0001$). B: Fxrα is activated by retinoids and some steroids. Transfection and dosing was performed as in A. Activation of Fxrα was measured as an average fold induction relative to control (DMSO). Asterisks indicate a statistically significant difference between control and treatment (*, $p<0.05$; ***, $p<0.0001$).

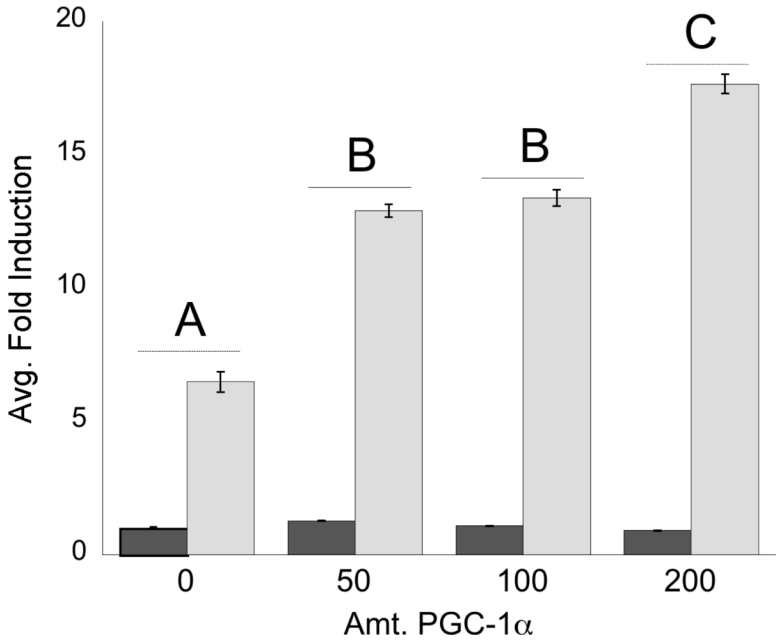

Figure 5. PGC-1α interacts with FxrαLBD/XgalX

PLHC-1 cells were seeded in 24-well plates at 2–3 × 10^5 cells/well and transfected with pRL-CMV, FxrαLBD/XgalX, 5XGal4-TATALuc, and a varying amount of pcDNA3.1–f:PGC1α (0–200 ng). The amount of DNA was equalized across wells by the addition of empty pCDNA3.1 plasmid. Cells were dosed for 24 hours with either DMSO or 1.0 μM GW4064. Activation was measured as an average fold induction relative to control (DMSO) for each amount of PGC-1α added. Letters correspond to statistically significant differences between treatments ($p<0.05$); treatments with the same letter are not statistically different from each other.

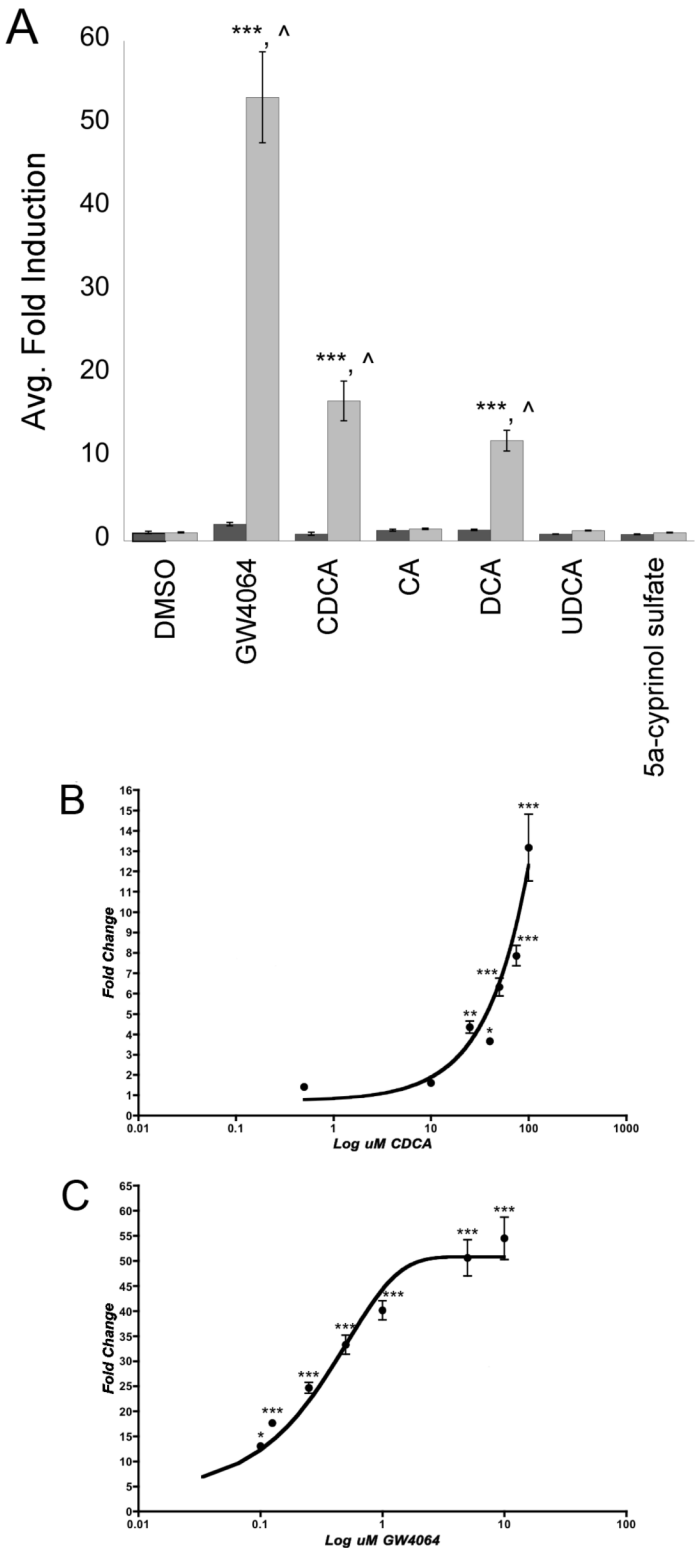

Figure 6. Fxrα2 interacts with IR-1 response elements, but not Fxrα1

A: CV-1 cells were seeded in 24-well plates at 1×10^5 cells/well and transfected overnight with pRL-CMV (normalizing plasmid), pcDNA3.1-f:PGC1α, $(hsp27EcRE)_2$-tk-Luc (reporter

plasmid), and either Fxrα1/pSG5 or Fxrα2/pSG5. Cells were dosed for 24 hours with a variety of BAs or DMSO only. Activation of each isoform was measured as an average fold induction relative to its control (DMSO, Fxrα1: dark gray; Fxrα2: light gray). Asterisks indicate a statistically significant difference between control and treatment (***, $p<0.0001$). Carats indicate a statistically significant difference between isoforms for that treatment (^, $p<0.01$). B and C: Fxrα2 is activated by CDCA (B) and GW4064 (C) in a dose-responsive fashion. CV-1 cells were seeded in 24-well plates at 1×10^5 cells/well and transfected as previously described in A. Activation was measured as an average fold induction relative to control (DMSO). Asterisks indicate a statistically significant difference between control and treatment (*, $p<0.05$; ***, $p<0.0001$).

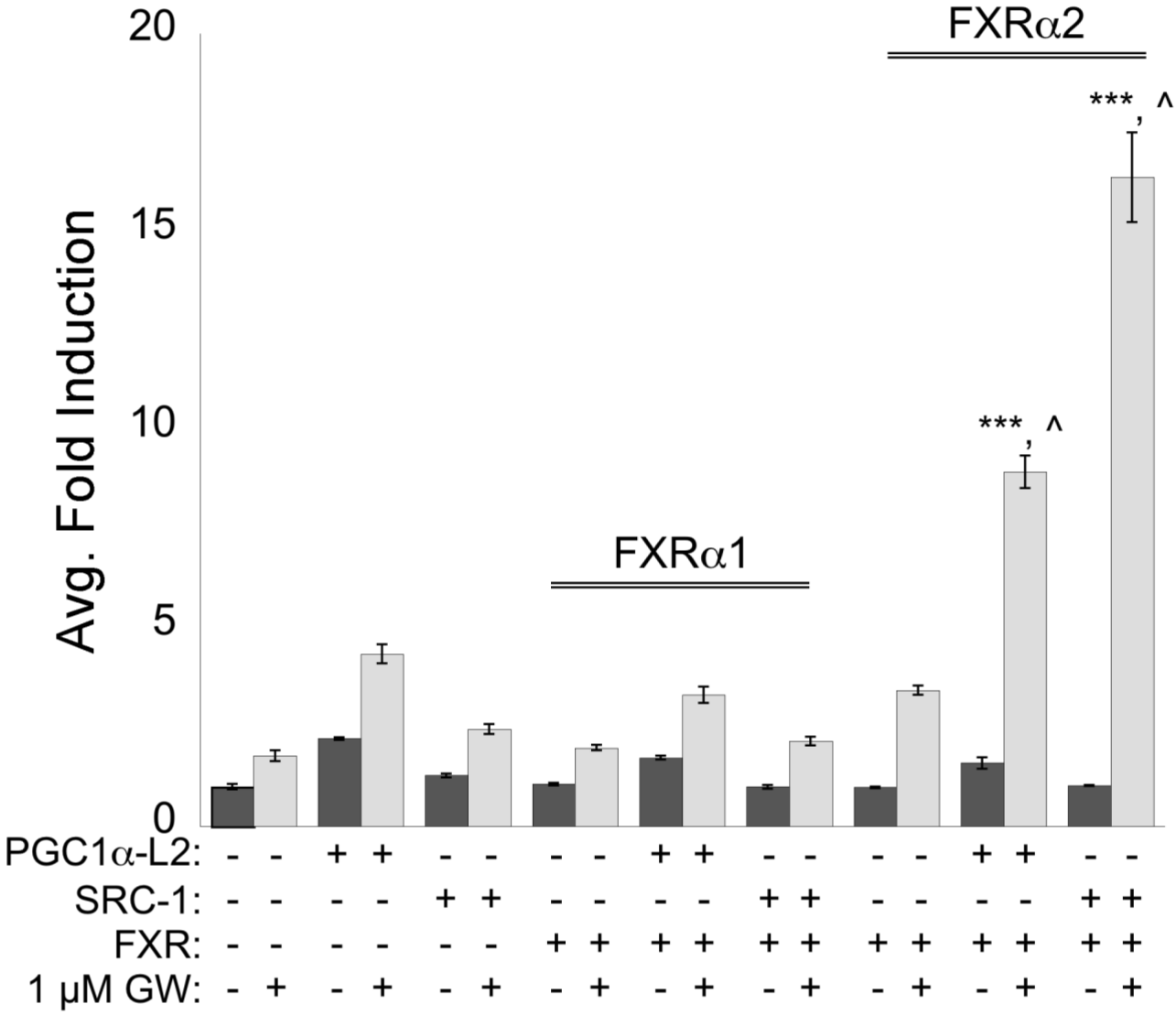

Figure 7. Mammalian two-hybrid assay with Fxrα1 or Fxrα2 and PGC-1α or SRC-1

CV-1 cells were seeded in 24-well plates at 1×10^5 cells/well and transfected overnight with pRL-CMV and 5XGal4-TATA-Luc, either pM.PGC-1αL2 or pM.SRC-1, and either Fxrα1/pSG5 or Fxrα2/pSG5. Cells were exposed to DMSO or 1 μM GW4064 in media for 24 h. FXRα response was measured via dual luciferase assays as described earlier. Data are represented as the mean fold induction of Fxrα normalized to control (DMSO for empty plasmids). Asterisks represent significant difference between control and treatment ($p<0.0001$) and carats represent significant difference between Fxrα1 and Fxrα2.

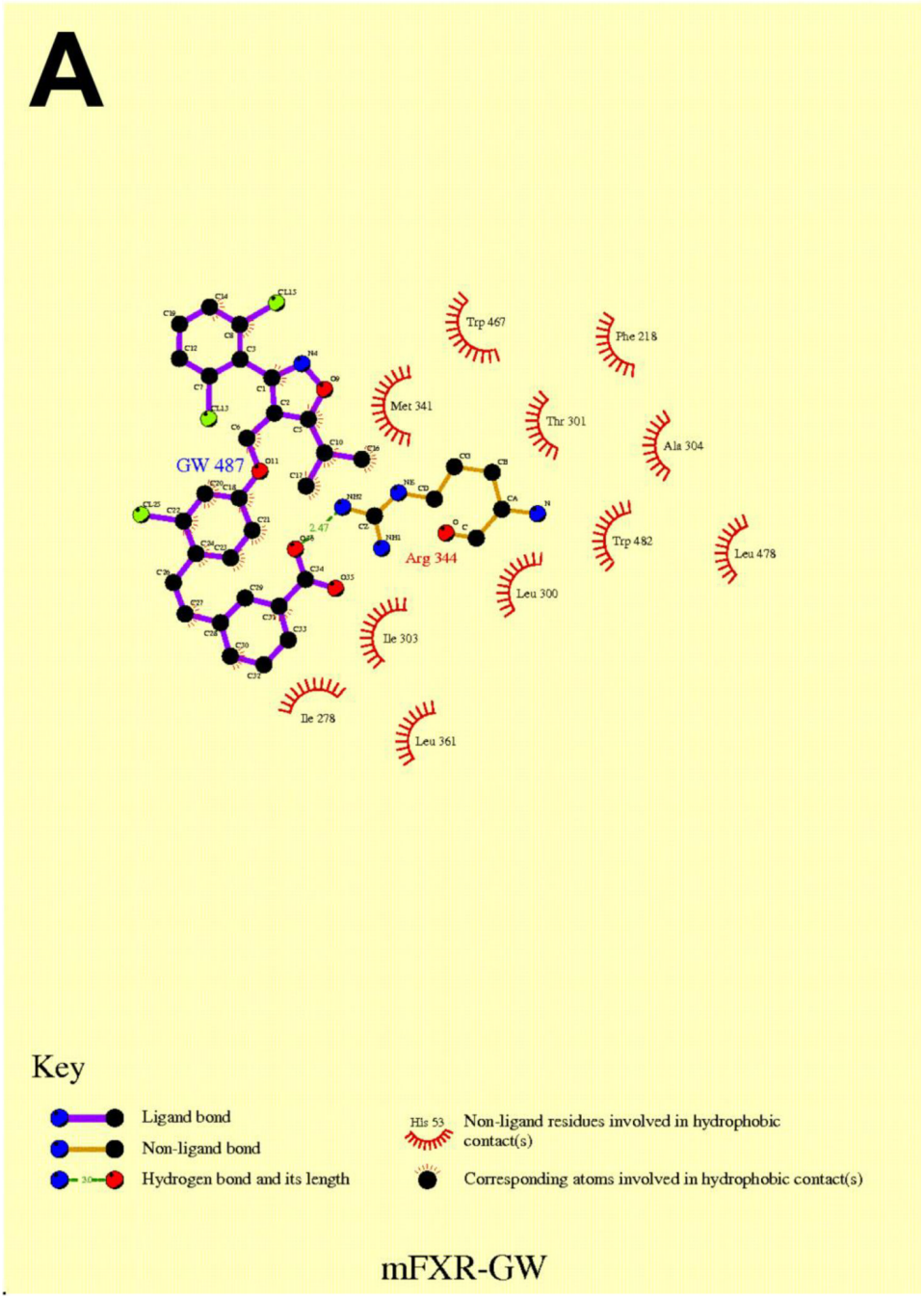

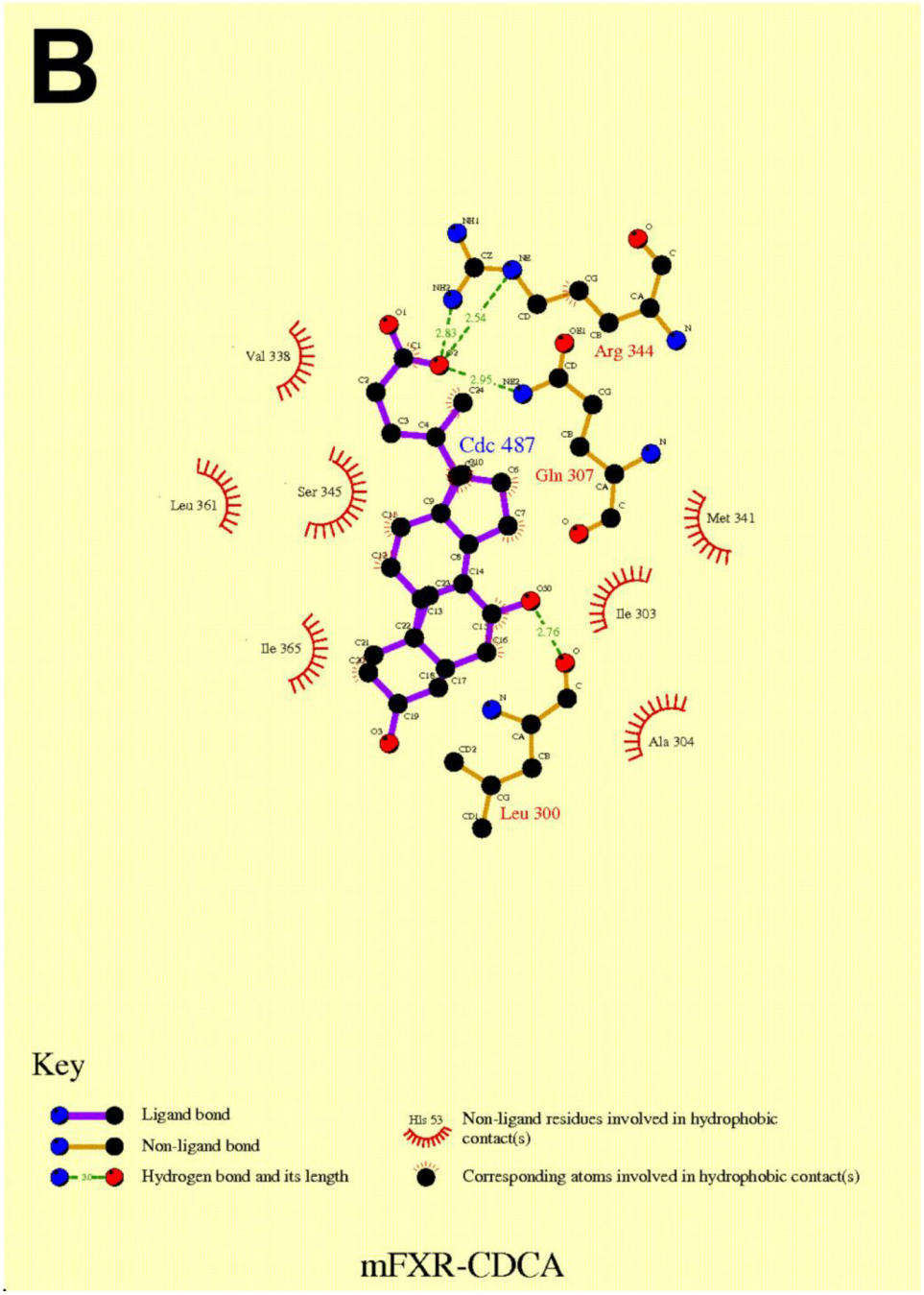

Figure 8. ***In silico*** **molecular modeling of Fxr*α*LBD with GW4064 (A) and CDCA (B)**

Table 1

List of primers

Primer Name	Sequence (5'→3')	Dir	Application
Fxrα1 Fwd	CCCTCCTGAATGAATGAGTGGGTGG	F	Cloning
Fxrα1 Rev	AGCAGAACCTCACTGCACATCCCAG	R	Cloning
5' RACE 1	CTCCTCCCCTTTGACCCGTCCAGCCTGCATCAT	R	5' RACE
5' RACE 2	CTGAGTGGAGTAAAATGGAGTGGAGGACATGG	R	5' RACE
EcoRI-Fxrα2 Fwd	CCCGAATTCATGGCCCTGGTACAGATGCAG	F	Cloning
BamHI-Fxrα2 Rev	AATGGATCCTCACTGCACATCCCAGATCTCACA	R	Cloning
KpnI-FxrαLBD Fwd	GGTACCGGCATGCTGGCAGAG	F	Cloning
BamHI-FxrαLBD Rev	GGATCCTCACTGCACATCCCA	R	Cloning
Fxrα1 qPCR F	CATCAGAGTACTTGAAGAAGATGTTGTCAGAGGACGG	F	qPCR
Fxrα1 qPCR R	CTCCTTCCGACATGGAGAAGTCATCGC	R	qPCR
Fxrα2 qPCR F	GAAGGGGAGATGGTTTTGTTGTAAAGGCTCAAAG	F	qPCR
Fxrα2 qPCR R	TCTTGAAGACTGCATCTGTACCAGGGCCAT	R	qPCR
18S RNA F	CCTGCGGCTTAATTTGACTC	F	qPCR
18S RNA R	GACAAATCGCTCCACCAACT	R	qPCR

Table 2

Homology of mammalian and non-mammalian FXRαLBDs (known and predicted)

Numbers in the table correspond to percent amino acid sequence identity.

	medaka	stickle	tetraodon	fugu	danio	chicken	cow	human	chimp	rat	mouse
medaka	100	85	84	84	80	72	70	70	70	70	70
stickle		100	85	87	80	72	67	68	68	67	68
tetraodon			100	95	78	71	67	68	68	67	68
fugu				100	79	72	68	69	69	69	69
danio					100	76	73	73	73	73	73
chicken						100	88	88	88	87	87
cow							100	94	94	95	95
human								100	100	95	95
chimp									100	95	95
rat										100	98
mouse											100